Journal of Colloid and Interface Science 528 (2018) 116–123

Contents lists available at ScienceDirect

Journal of Colloid and Interface Science

journal homepage: www.elsevier.com/locate/jcis

Regular Article

Effect of protein adsorption on the radial wicking of blood droplets in paper

Michael J. Hertaeg [a], Rico F. Tabor [b], Gil Garnier [a,*]

[a] BioPRIA and Department of Chemical Engineering, Monash University, Clayton, VIC 3800, Australia
[b] School of Chemistry, Monash University, Clayton, VIC 3800, Australia

GRAPHICAL ABSTRACT

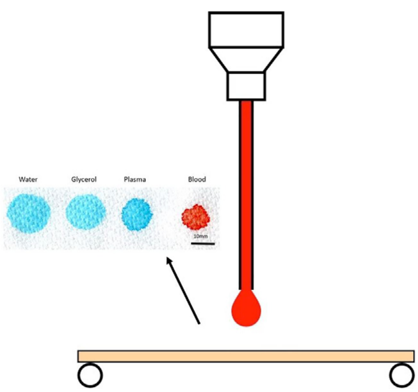

ARTICLE INFO

Article history:
Received 4 April 2018
Revised 9 May 2018
Accepted 14 May 2018
Available online 23 May 2018

Keywords:
Blood
Protein
Radial wicking
Protein adsorption
Stain area
Paper
Biodiagnostic

ABSTRACT

Hypotheses: (1) The equilibrium size and characteristics of a radially wicked fluid on porous material such as paper is expected to be dependent on the fluid properties and therefore could serve as a diagnostic tool. (2) The change in wicked stain size between biological fluids is dependent on a change in solid-liquid surface interfacial energy due to protein adsorption.
Experiments: Sessile droplets of increasing volume of blood, its components, and model fluids were deposited onto paper and the equilibrium stain size after coming to a halt was recorded. The contact angle of fluid droplets on model cellulose surfaces was measured to quantify the effect that blood protein adsorption at the solid-liquid interface has on radially wicked equilibrium size. Finally the significance of droplet evaporation for the time scale of interest was analysed.
Findings: The final stain area of all fluids tested on paper scales remarkably linearly with droplet volume. Different fluids were compared and the gradient of this linear relation was measured. Model fluids varying in surface tension and viscosity all behave similarly and exhibit a constant gradient. Blood and its components produce smaller stains, demonstrated by lower gradients. The gradient is a function of protein concentration, thus the mechanism of this phenomenon was identified as protein adsorption at the cellulose-liquid interface. The slope of the area/volume relationship for droplets is an important quantitative mechanistic variable.

* Corresponding author.
E-mail address: Gil.Garnier@monash.edu (G. Garnier).

https://doi.org/10.1016/j.jcis.2018.05.037

1. Introduction

The wicking of fluids through porous media is of fundamental importance in many processes and applications such as printing, textiles, agriculture and more recently the medical field for its applications in paper based blood diagnostic tools [1,2].

Blood is a suspension of cells that are weakly electrostatically stabilised in plasma, the liquid component of blood. Plasma consists mostly of water (90 wt%), proteins (approximately 6 wt%) and a small amount of lipids, carbohydrates and electrolytes [3]. There are different types of proteins in blood of which the most abundant are albumin (38.7 g/L) [4], globulin (25 g/L) and fibrinogen (3 g/L) [3]. The composition and protein concentrations in blood vary greatly as a function of health as well as natural variation among populations [5,3,6]. Many blood proteins are surface active and readily adsorb onto surfaces [7]. There are three main types of cells in blood: erythrocytes (red cells), lymphocytes (white cells) and platelets. The majority of cells in blood are red blood cells. Healthy red blood cells are biconcave disks approximately 8 μm in diameter and 3 μm in thickness [8]. The shape, abundance and mechanical properties (deformation) of these cells are responsible for the unique viscoelastic and shear thinning behavior of blood [9]. By centrifugation the majority of cells can be removed from blood allowing the analysis of solely the plasma component. Although plasma exhibits weak viscoelastic properties [10], most analyses assume Newtonian behavior to no significant loss in accuracy. By testing plasma instead of whole blood the effect of protein adsorption can be isolated from the non-Newtonian properties of blood cells as a suspension (shear thinning, viscoelasticity and granularity).

The radial wicking of a drop has been studied previously [11–15]. However all previous studies have considered highly idealised systems ignoring evaporation and the complex properties of multicomponent systems. This study aims to identify the parameters and phenomena controlling the final stain area achieved by a single droplet of blood radially wicking onto paper. This is of direct interest in the development of blood diagnostics for several reasons. The surprising reproducibility and sensitivity of results suggest that drop stain analysis can serve as a convenient and inexpensive method to identify fluid properties. Whether these property changes are caused by protein content, specific antibody-antigen reaction or hematocrit levels will determine the nature of the sensor. The effect of protein concentration is examined here; however, this type of analysis is applicable to many sensing applications. Further a robust fundamental knowledge of the blood stain/volume relationship on paper/porous media will allow more sensitive, faster and more accurate diagnostic methods to be developed and guide the optimisation of existing devices. This study is also relevant to any system involving the contact or deposition of a wetting liquid over a porous material.

2. Experimental section

2.1. Materials

Tests were performed on Kimberly Clark Scott hand towel (4419) and Whatman 41 filter paper. Wet, dry and oven dried (O.D) weights of 100 cm^2 sections of paper are given in Table 1. The wet and dry thicknesses were also measured. Analytical grade glycerol, and ethanol were purchased from Merck, and Thermo Fisher Scientific, respectively. BSA (bovine serum albumin) solutions were diluted from 30% (wt/v) solutions from BioCSL, PBS (phosphate buffered saline) was made to 0.9 wt% with tablets from Sigma. Human blood with EDTA anti-coagulant was provided by the Australian Red Cross following established best ethics practice. Deionized water for tests and dilutions was purified from tap water with a Direct-Q water purification system to a minimum resistivity of 18.2 MΩ cm.

2.2. Methods

2.2.1. Paper characterisation

Paper oven dry (O.D) weight was measured using TAPPI standard 412 by placing samples in a 105 °C oven until weight stabilised. The weight at this point was recorded. The given values are the mean of 3 recordings for each type of paper. Dry Weight was measured using TAPPI standard 402, where the weight of the samples after equilibration in 23 °C 50% relative humidity (RH) conditions for at least 24 h was measured. The values reported are the mean of 6 recordings for each type of paper. Wet weight was determined using a variation of testing standard TAPPI 441. This involved submersing the paper in water for 2 h, then pressing each between two pieces of blotting paper with 2 passes of a 10 kg roller to remove excess water. The paper was then weighed. This process was repeated until weight stabilised. The values for wet weight presented in Table 1 are the mean of 3 recordings for each type of paper. Wet and dry thicknesses were measured using a L & W micrometer. Thickness values are the mean of 10 measurements.

2.2.2. Equilibrium stain size

Reproducible droplets of volume ranging from 2 to 40 μL were created with an adjustable needle and a syringe pump (Fig. 1a). The syringe pump was used to provide a constant flow rate to the needle which created repeatable small drops. Drop size could be controlled by needle geometry. These droplets were directed onto a paper surface that was suspended in 23°C 50% relative humidity (RH) air. Setup took sufficient time to assume fluids were at room temperature during tests. The paper was then imaged using an Epson perfection V370 office scanner and analysed to give the area of each stain. Droplets were recorded in groups of at least 7 onto one piece of paper that was moved between each drop. The volume of the created droplets was measured 4 times before and after being directed onto paper to ensure the drops' volume remained a constant. Prior to tests with biological fluids, needles were soaked for at least 2 h in the fluid to be tested. This was to ensure protein adsorption onto the needle's surface was at equilibrium which improved the uniformity of drops. The difference in area between stains and the variation in measured drop volume is given as error bars in Fig. 2a and b. All property values were found in literature [16–20], except the viscosity and surface tension of blood plasma and BSA solutions, these were measured with an Ostwald viscometer and a pendant drop surface tensiometer [21]. The

Table 1
Paper properties.

Paper	O.D weight (g)	Std Dev (g)	Dry weight (g)	Std Dev (g)	Wet weight (g)	Std Dev (g)	Dry thickness (μm)	Std Dev (μm)	Wet thickness (μm)	Std Dev (μm)
Hand towel	0.2558	0.0030	0.2671	0.0031	0.5537	0.0180	98	2	76	2
Filter paper	0.8537	0.0065	0.8794	0.0174	1.8086	0.0208	226	5	218	5

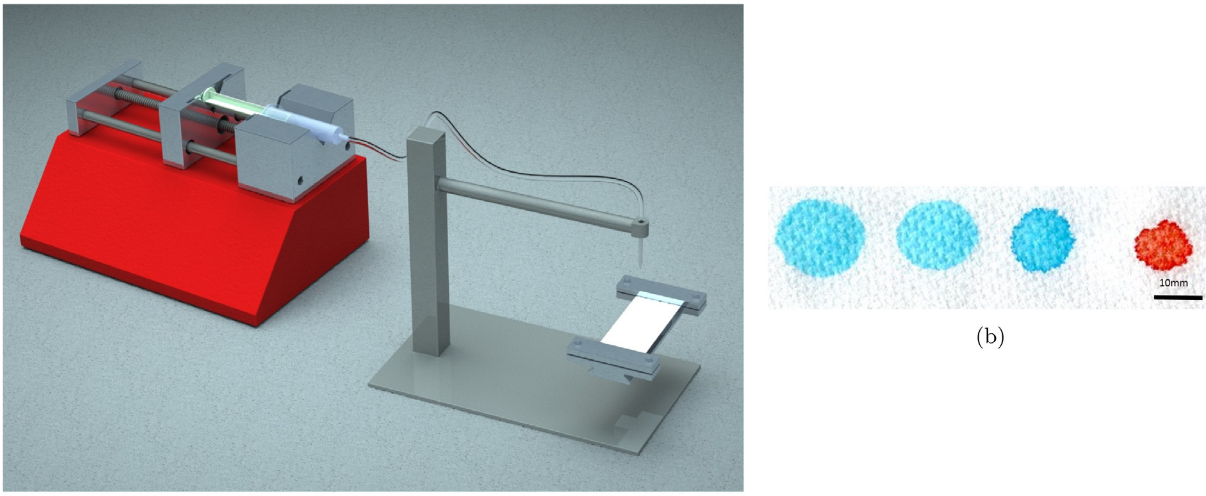

(a) (b)

Fig. 1. (a) Diagram of the experimental system depositing sessile droplets of controlled volume on paper. (b) Stains produced from 8 μL droplets of different fluids on paper at identical ambient conditions. From left to right: 25% glycerol, 20% Ethanol, plasma and whole blood. Colourless fluids have blue dye (3 wt%) added to aid visualisation. (For interpretation of the references to colour in this figure legend, the reader is referred to the web version of this article.)

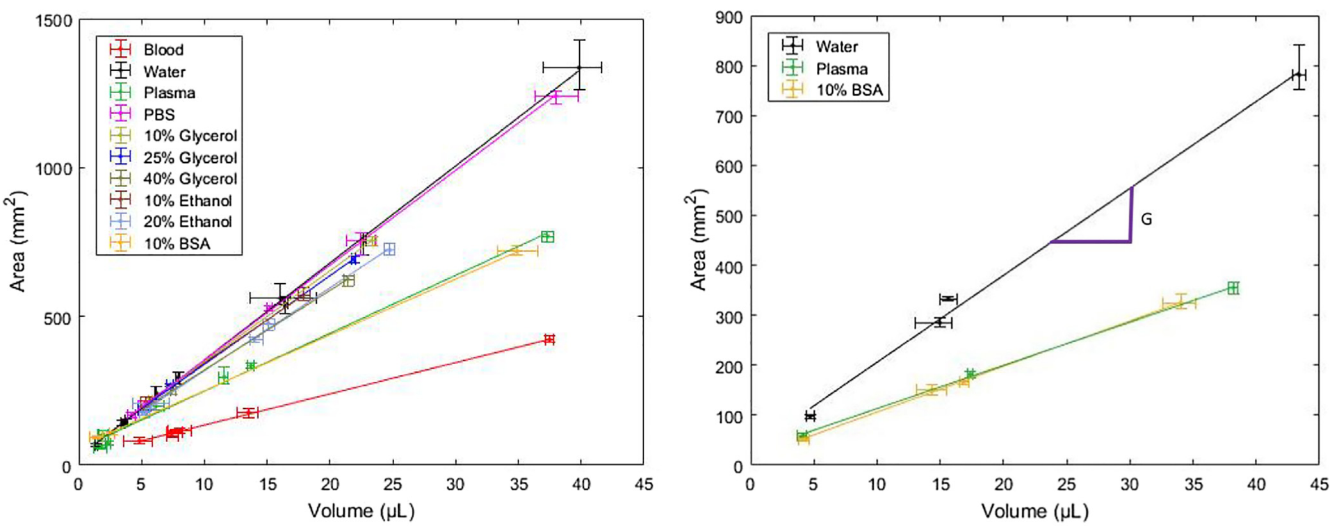

(a) (b)

Fig. 2. Effect of initial droplet volume on equilibrium stain area on paper hand towel for blood components and model fluids. The average, minimum and maximum area/volume of at least 7 droplets are shown. All measurements were performed at 23 °C 50% RH. (a) all fluids on paper hand towel and (b) a selection of fluids on filter paper.

density of BSA solutions, plasma and PBS were measured using a Mettler Toledo TLE balance and Eppendorf Pipette.

Surface tension results were complicated by the dynamic surface tension of plasma and BSA [22]. This surface tension variation with time has not been well studied and it is unclear how the surface tension of blood and blood components will change during wicking. For the purpose of this study, highly accurate surface tension data was not required, therefore the average recorded surface tension over a relevant time scale (10–15 s) is reported.

2.2.3. Contact angle measurements

Cellulose thin films were prepared by regenerating spin coated cellulose acetate as previously described [23,24]. A 0.5 wt% solution of cellulose acetate was spin coated onto a plasma cleaned glass slides at 2000 RPM for 20 s. These slides were then regenerated from cellulose acetate to cellulose by soaking in a 0.5% sodium methoxide solution for 10 h. The advancing contact angle was determined using a dataphysics OCA35 contact angle instrument by taking measurements at several points as liquid was pumped into the drop at a rate of 20 μL/s. For each batch of cellulose films, this test was repeated at least three times for each fluid, and three batches of cellulose films were tested. Roughness measurements using a JPK Nanowizard 3 atomic force microscope were completed on 4 of the cellulose surfaces; the roughness value reported is the mean of these 4 values.

2.2.4. Drying time measurement

Tests were completed by suspending a paper towel sample in a digital scale and recording the weight as a function of time. This allowed the rate of evaporation to be measured. The drop size used was 8 μL and the tests were performed at 23 °C 50% relative humidity (RH). The fluids tested were PBS (phosphate buffered saline), 10% BSA (bovine serum albumin), water and plasma.

3. Results

Droplets varying in volume were deposited on paper and the area of the stain at equilibrium was measured for a series of fluids. Blood, blood components and model fluids varying in viscosity and surface tension were tested under standard humidity and temperature conditions. The size, shape, perimeter fractal and colour intensity distribution of the stains on paper vary among the different fluids of the same volume (Fig. 1b). However, size is the most important variable of these stains. The average, maximum and minimum values for stain size and drop volume for a minimum of 7 replicates are shown in Fig. 2a and b. Linear trend lines are fitted for reference.

3.1. Equilibrium stain size

Fig. 2a shows the equilibrium stain size for all tested fluids deposited on paper hand towel, where Fig. 2b shows a selection of these fluids on filter paper. The stain area of a droplet on paper is surprisingly reproducible and scales linearly with volume. All fluids tested show a similar linear trend however with a shift in slope or gradient. At constant drop volume, whole blood creates the smallest stain, followed by plasma. The stain area at equilibrium can be expressed as:

$$A = GV + C \tag{1}$$

where A is the equilibrium area (mm^2), V is the drop volume (μL), G is the gradient of stain area to drop volume ($\frac{1}{mm}$) and C is a constant (mm^2). The calculated value of C range between 74 and 20 mm^2. This value is slightly larger than the average error in area measurements and is always positive.

The gradient G varies significantly between the different fluids and papers. The gradient values for the model fluids on hand towel as well as the fluid properties are presented in Table 2. The gradient value does not correlate with the fluid surface tension or viscosity significantly.

3.2. Effect of protein concentration

Fig. 3a shows the gradient values for solutions of different concentrations of BSA on the paper hand towel. These results were collected in the same way as results in Fig. 2a and b. The gradient of the lines is plotted against BSA concentration. The gradient decreases in a roughly inverse square root fashion with BSA concentration. A faster changing gradient is seen at lower BSA concentrations. This might indicate some adsorption surface saturation mechanism.

3.3. Contact angle measurements

As different and lower gradients are only seen with biofluids on paper, wetting experiments were performed on smooth cellulose films to understand the effect of wetting. Fig. 4 shows the advancing contact angle of a series of selected fluids on model cellulose surfaces. Histograms are presented to visually highlight a statistically significant shift in the mean contact angle despite a high amount of variability in results. This variability has a physical

Table 2
Fluid properties at 23 °C effecting wicking behavior [16–20].

Solution	Concentration (*wt*%)	Density (kg/m^3×10^3)	Surface tension (mN/m)	Viscosity (mPa s)	Surface tension/Viscosity (m/s)	Gradient (1/m × 10^3)
Water	100%	1.00 [16]	72.31 [28]	0.93 [16]	77.75	32.6
Glycerol	10%	1.02 [18]	71.97 [19]	1.21[18]	59.48	30.5
Glycerol	25%	1.06 [18]	70.95 [19]	1.92[18]	36.95	29.8
Glycerol	40%	1.10 [18]	69.61 [19]	3.40[18]	20.47	26.7
Ethanol	10%	0.96 [17]	39.29[17]	1.96[17]	20.0	28.8
Ethanol	20%	0.93 [17]	32.27[17]	2.52[17]	12.8	27.9
Plasma	100%	1.01	45	1.74	25.9	19.4
BSA	10%	1.01	40	0.93	43.0	18.7
PBS		1.00	72.2 [20]	1.00 [20]	72.2	31.8

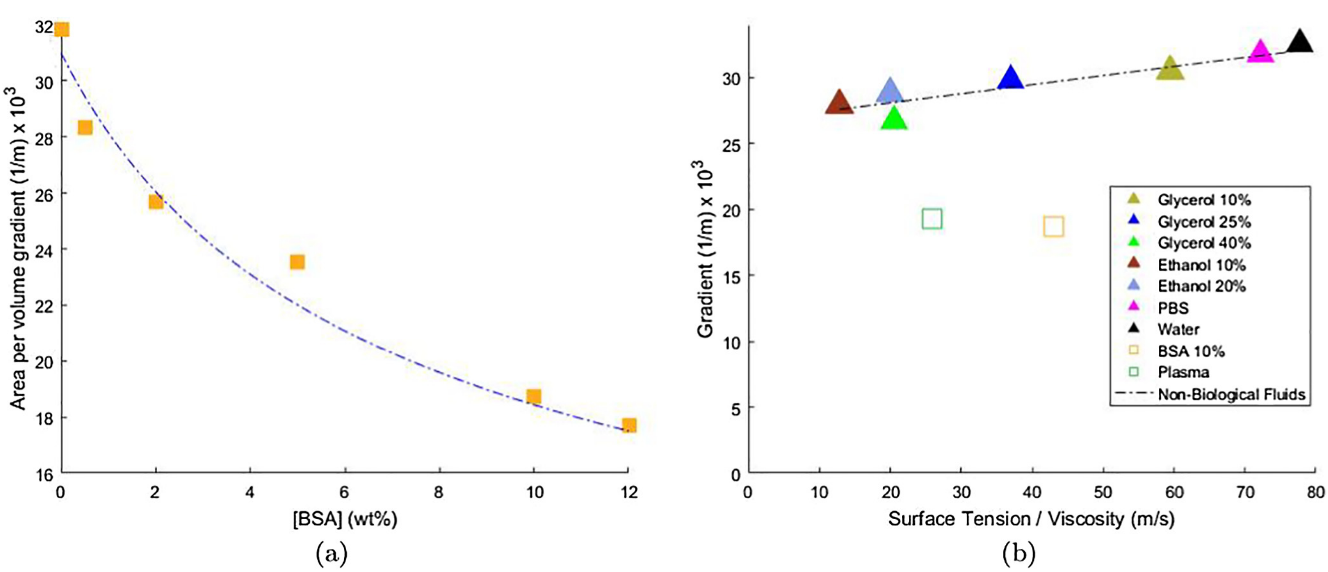

Fig. 3. (a) The droplet area/volume gradient plotted as a function of protein concentration for a series of BSA solutions. A trend line has been drawn to guide the eye. (b) Effect of surface tension to viscosity ratio on the stain area to drop volume gradient. A linear trend line is fitted for non-biological fluids. Biological fluids do not follow this trend.

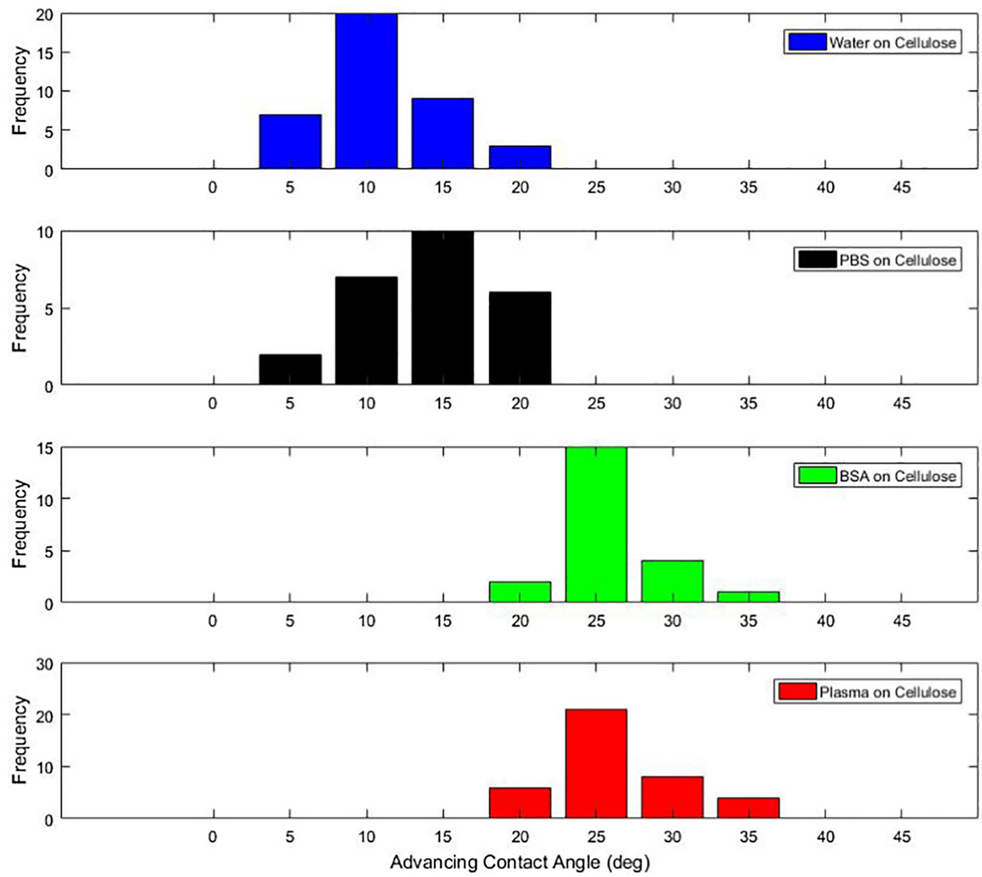

Fig. 4. Histogram of advancing contact angle measurements for water, PBS and biological fluids on cellulose films.

meaning as it quantifies both the chemical and physical heterogeneity of the cellulose films. There is a similar increase in the mean contact angle for biological fluids when compared to non biological fluids.

3.4. Time scale of evaporation

To simplify matters it was intended to study wicking under conditions independent of liquid evaporation. This was achieved by testing in a conditioned laboratory at 23 °C and 50% relative humidity (RH). The effect of droplet evaporation was analysed by measuring the relative weight of a drop deposited onto paper during evaporation. For the time period required for stain growth to fully stop (5–15 s) all fluids had evaporated by less than 10%. Water and PBS evaporate at the same rate, while plasma and BSA solutions evaporate similarly but at a slower rate (Fig. 5).

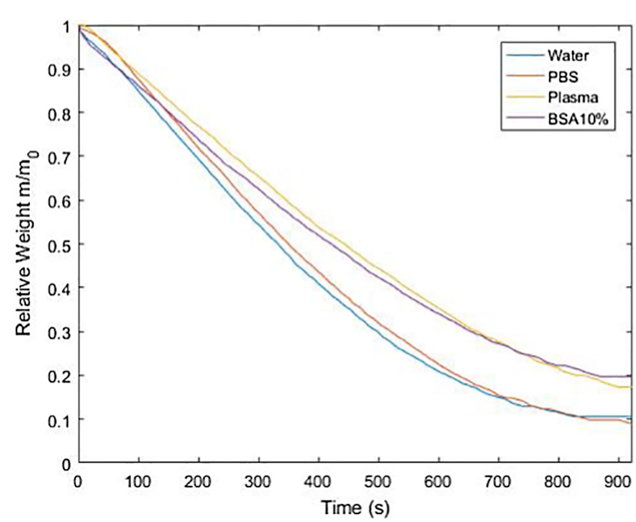

Fig. 5. Weight of 8 μL drops of tested fluids on paper in 23 °C 50% relative humidity air. Y axis is normalised by initial drop weight. All show limited drying at a time where the stain growth was observed to stop, approximately 11 s. These results are shown in Fig. 5

4. Discussion

4.1. Equilibrium stain size

Fig. 2a and b show a clear distinction between the wicking behavior of biological and non-biological fluids on paper. Despite large variations in both surface tension and viscosity between water, ethanol and glycerol solutions, there is no significant change in gradient. This is surprising as previous research on non-equilibrium radial spreading has shown a strong dependency on the ratio $\frac{\gamma}{\eta}$ [12,14], although this is not directly comparable to equilibrium results. Fig. 3b shows the effect of the $\frac{\gamma}{\eta}$ ratio on the gradient of the equilibrium stain area to drop volume curve with all fluid properties presented in Table 2. There is a slight dependence of the gradient on the $\frac{\gamma}{\eta}$ ratio for non-biological fluids and a linear function was arbitrarily fitted. Plasma and 10% BSA solution do not follow the trend of model fluids. Table 2 also shows that the gradient parameter does not directly scale with either viscosity or surface tension. Although there may be a slight dependence of the stain area/drop volume gradient with the $\frac{\gamma}{\eta}$ ratio, there is another property that presents itself in blood plasma that is far more dominant. This extreme variation in stain sizes between plasma and model fluids was not reported by Li et al. in their experiments with porcine plasma on cotton 'T-shirt' fabric[25]. The gradient for blood is significantly smaller than all tested fluids. The stain area of blood is on average 55% that of plasma using droplets of identical volumes. This finding corroborates the study of Li et al. with porcine blood/plasma who further reported the blood to plasma stain ratio to be equal to one minus the average hematocrit value of blood [25]. The authors relied on this observation to justify the assumption that it is only the volume of the plasma component that determines stain size. Although the value of this repeatable stain size ratio between blood and plasma is intriguing, it is unlikely that the red blood cells have no effect on the wicking process. Other causes of the smaller stain size for blood could include blood cells form blockages in the smaller pores of paper, or electrostatic repulsion between the negatively charged red blood cells[26] and the anionic cellulose [27]; however this is unlikely to be significant due to the micro scale of red blood cells.

Stains on different papers can be compared by defining a new variable, the paper ratio factor (PRF). This is calculated as the gradient of the stain area to volume relationship on a certain paper, divided by the gradient of the same fluid on a different reference paper (Eq. (2)). Table 3 compares the PRF values on hand towel and filter paper for 3 fluids. If the two papers were to behave identically, simple volume conservation analysis reveals that the PRF should be equal to the ratio of the two paper thicknesses. This ratio was measured by micrometer and found to be 2.26.

$$PRF = G_{HandTowel}/G_{FilterPaper} \tag{2}$$

Although plasma and BSA have PRF factors close to 2.26, water shows a slightly lower than expected ratio. This implies that water and biological fluids are affected differently by the change in paper properties.

Schuchard et al. reported fiber swelling to be an important parameter to consider for wicking in cellulose networks [29]. All fluids used in this study are water-based and therefore will swell cellulose; however, it is not clear if there is a difference in swelling among fluids and whether this would cause a change in stain area. This could be the cause of the shifts in PRF value between fluids as paper type may affect the extent of fiber swelling.

4.2. Effect of evaporation

The linearity of the equilibrium stain area with drop volume relationship (Fig. 2a) implies the absence of any significant evaporation. If evaporation was taking place, a plateau would be expected at the higher drop sizes. This is further shown by drying time experiments in which the weight after fluid contact with paper was measured with time. No significant drying occurs in the time frame of wicking, which range between 5 and 15 s in this study. Therefore evaporation is insignificant for the system studied. Measurements with water, plasma, PBS and BSA solutions all show similar behavior.

This differs from expectations from literature. Gilespie [13] predicted that a wicked stain equilibrium area would only be detectable when evaporation is significant. It might be possible that the measured apparent equilibrium position is actually a state where the front is moving so slowly that its motion is unobservable and the final position is the effect of drying after a significant time.

Nilghaz et al. [30] demonstrated that coffee rings [31] form on paper in some situations. As the mechanism of coffee ring formation is dependent on a pinned outer edge [32], and the effects of surface pinning are not included in models that predict indefinite spreading, pinning may be a determining factor in stain equilibrium size.

Table 3
Paper ratio factor (no unit). Filter paper is used as reference paper.

Fluid	PRF
Water	1.87
Plasma	2.25
10% BSA	2.06

4.3. Wetting mechanism

Advancing contact angle measurements were performed on model cellulose films. The contact angle data can be used with the Young equation [33] (Eq. (3)), to determine the interfacial energy at the solid liquid interface. Eq. (4) accounts for surface roughness [34]. The value for the cellulose-air interfacial energy γ_{sv} used is 69.0 mN/m. This value is the mean of the two testing methods for the surface energy of untreated cellulose fibers by Westerlind and Berg [35] and is very close to the value also found by Niegelhell et al. [36]. The roughness used in calculations was measured by atomic force microscopy to be 1.16. Roughness is defined as the real surface area divided by the surface area of a smooth surface of the same dimensions.

$$\gamma_{sv} = \gamma_{sl} + \gamma_{lv}\cos\theta \tag{3}$$

where γ_{sv}, γ_{sl} and γ_{lv} are the solid-vapour, solid-liquid and liquid-vapour surface tensions respectively.

$$\cos\theta_{app} = r\cos\theta_r \tag{4}$$

where θ_{app} is the apparent measured contact angle, r is the roughness of the substrate and θ_r is the real contact angle that can be used in the Young equation. The solid-liquid interfacial energies calculated are presented in Table 4. Results from PBS are calculated to demonstrate the negligible effect of ionic strength on wetting.

The equilibrium stain size of 0% BSA or 100% PBS are similar to tests with water, which shows that the effect of salinity is negligible.

4.4. Protein adsorption

Surface energy measurements show the solid liquid surface energy to be significantly raised by high protein concentrations in the droplet solution. Fluids exhibiting similar stain sizes, such as 10% BSA and plasma also have very similar surface energies. This suggests a relationship between stain size and the solid-liquid interfacial energy which is affected by protein content in the fluid. This is most likely caused by protein adsorption onto the cellulose surface.

The adsorption of BSA and human immunoglobulin G onto cellulose was previously demonstrated [7]. This adsorption of blood proteins was shown to make cellulose more hydrophobic after aging and drying [23]. This augmented hydrophobicity is caused

Table 4
Liquid solid interfacial energy measured from wetting experiments for the different fluids on cellulose films.

Fluid	Mean advancing contact angle (degrees)	Solid-liquid interfacial energy (mN/m)
Water	13.5	8.4
PBS	16.6	9.3
BSA 10%	28.4	38.6
Plasma	28.9	35.0

by an increase in solid-liquid interfacial energy at the cellulose interface due to a protein conformation change. The increased solid-liquid interfacial energy calculated here is likely caused by a similar mechanism although contact angle measurements were performed with the protein solution, not water after drying as in previous studies. An increase in cellulose-fluid interfacial energy would cause a decrease in stain area as the formation of such an interface is energetically unfavorable.

As a wicking system is in motion the transportation of solution components is not necessarily homogeneous due to adsorption and diffusive variations. Such variations can effect wicking of surfactant solutions [37]. The surface energies calculated for static drops in equilibrium presented may not directly translate to transient wicking analysis. It is also unknown how the addition of protein will affect fiber swelling.

Interpolating from the trend in Fig. 3a, plasma behavior is similar to a solution having a BSA concentration of 8.3%. This value differs from the average concentration of albumin in human plasma which is 3.9% [4], with normal values ranging from 3.2% to 4.5% [5]. Although albumin concentration is likely to be a factor affecting plasma equilibrium wicked area, it is not the only factor.

Albumin represents only 60–65% by weight of blood plasma proteins [6]; there are many other blood proteins capable of adsorbing onto cellulose [7]. The concentration of all proteins in plasma is approximately 6.2%. Comparing this value to the plasma similar BSA solution concentration (8.3%) reveals that either non-albumin proteins effect equilibrium on a per weight basis more than albumin, or there is another factor that has not been investigated, such as the competitive binding of phosphate ions from PBS [38].

5. Conclusion

A series of small droplets of blood and model fluids were deposited onto paper and the stain area to drop volume was measured for droplets of increasing volume. The model fluids studied consist of a selection of simple fluids varying in surface tension and viscosity, as well as blood plasma and protein solutions of different concentrations. The stain area-droplet volume relationship was studied. This was performed under controlled conditions (23 °C and 50% RH) under which evaporation was negligible. To better distinguish the effect of wetting from radial wicking in a porous material, the contact angle of plasma and water were measured over smooth cellulose films.

The area of the stain achieved by the radial wicking of a droplet of controlled volume deposited onto paper is very reproducible. Stain area scales linearly with droplet volume. The slope of the stain area-droplet volume relationship (gradient) is indicative of the fluid composition and the paper structure. The gradient is however nearly independent of fluid viscosity and surface tension. Blood has the lowest gradient, followed by plasma, protein solutions and the model simple fluids each having nearly identical slopes. This different behaviour was attributed to the adsorption of protein onto paper, affecting the solid-liquid (γ_{sl}) interfacial energy. The protein content of BSA solutions and blood was found to strongly effect the gradient and therefore the equilibrium stain size. This is due to the increase in surface energy that occurs after protein adsorption onto the cellulose fluid interface. Previous studies have shown that the ratio of surface tension to viscosity is a critical parameter for situations under non-equilibrium wicking conditions [12–14]. However, our results were found to be almost independent of the ratio. The paper ratio factor (PRF) is proposed as a new measure of the relative stain sizes in different papers and is compared to the ratio of thicknesses to identify effects from paper structure.

The reproducibility of stain area-droplet volume on paper, its ease of measurement combined with the slope (gradient) being a function of fluid properties all make blood stain analysis very attractive for diagnostic applications. Blood stain analysis could become the basis for a new generation of high throughput and very fast blood diagnostic systems.

Acknowledgments

This research was funded by an ARC Linkage grant (LP160100544) and Haemokinesis.

References

[1] M. Al-Tamimi, W. Shen, R. Zeineddine, H. Tran, G. Garnier, Validation of paper-based assay for rapid blood typing, Anal. Chem. 84 (3) (2012) 1661–1668.
[2] W. Then, M. Li, H. McLiesh, W. Shen, G. Garnier, The detection of blood group phenotypes using paper diagnostics, Vox sanguinis 108 (2) (2015) 186–196.
[3] R. Chen, L. Zhang, D. Zang, W. Shen, Blood drop patterns: formation and applications, Adv. Colloid Interface Sci. 231 (2016) 1–14.
[4] D.J. Greenblatt, Reduced serum albumin concentration in the elderly: a report from the boston collaborative drug surveillance program, J. Am. Geriatr. Soc. 27 (1) (1979) 20–22.
[5] B.N. Azab, V.R. Bhatt, S. Vonfrolio, R. Bachir, V. Rubinshteyn, H. Alkaied, A. Habeshy, J. Patel, A.I. Picon, S.W. Bloom, Value of the pretreatment albumin to globulin ratio in predicting long-term mortality in breast cancer patients, Am. J. Surg. 206 (5) (2013) 764–770.
[6] M. Otagiri, V.T.G. Chuang, Albumin in Medicine: Pathological and Clinical Applications, Springer, 2016.
[7] H. Orelma, I. Filpponen, L.-S. Johansson, J. Laine, O.J. Rojas, Modification of cellulose films by adsorption of CMC and Chitosan for controlled attachment of biomolecules, Biomacromolecules 12 (12) (2011) 4311–4318.
[8] M. Thiriet, The Biology and Mechanics of Blood Flows, Springer, 2008.
[9] A. Copley, G. Stainsby, Flow Properties of Blood, Pergamon Press, 1960.
[10] M. Brust, C. Schaefer, R. Doerr, L. Pan, M. Garcia, P. Arratia, C. Wagner, Rheology of human blood plasma: viscoelastic versus newtonian behavior, Phys. Rev. Lett. 110 (7) (2013) 078305.
[11] A. Borhan, K. Rungta, On the radial spreading of liquids in thin porous substrates, J. Colloid Interface Sci. 154 (1) (1992) 295–297.
[12] D. Danino, A. Marmur, Radial capillary penetration into paper: limited and unlimited liquid reservoirs, J. Colloid Interface Sci. 166 (1) (1994) 245–250.
[13] T. Gillespie, The spreading of low vapor pressure liquids, J. Colloid Sci. 13 (1958) 32–50.
[14] E. Kissa, Capillary sorption in fibrous assemblies, J. Colloid Interface Sci. 83 (1) (1981) 265–272.
[15] A. Marmur, Penetration and displacement in capillary systems of limited size, Adv. Colloids Interface Sci. 39 (1992) 13–33.
[16] J. Kestin, M. Sokolov, W.A. Wakeham, Viscosity of liquid water in the range- 8 c to 150 c, J. Phys. Chem. Ref. Data 7 (3) (1978) 941–948.
[17] I.S. Khattab, F. Bandarkar, M.A.A. Fakhree, A. Jouyban, Density, viscosity, and surface tension of water+ ethanol mixtures from 293 to 323k, Korean J. Chem. Eng. 29 (6) (2012) 812–817.
[18] M.L. Sheely, Glycerol viscosity tables, Ind. Eng. Chem. 24 (9) (1932) 1060–1064.
[19] K. Takamura, H. Fischer, N.R. Morrow, Physical properties of aqueous glycerol solutions, J. Petrol. Sci. Eng. 98 (2012) 50–60.
[20] H. Tavana, C.-H. Kuo, Q.Y. Lee, B. Mosadegh, D. Huh, P.J. Christensen, J.B. Grotberg, S. Takayama, Dynamics of liquid plugs of buffer and surfactant solutions in a micro-engineered pulmonary airway model, Langmuir 26 (5) (2009) 3744–3752.
[21] J.D. Berry, M.J. Neeson, R.R. Dagastine, D.Y. Chan, R.F. Tabor, Measurement of surface and interfacial tension using pendant drop tensiometry, J. Colloid Interface Sci. 454 (2015) 226–237.
[22] S. Zaitsev, Dynamic surface tension measurements as general approach to the analysis of animal blood plasma and serum, Adv. Colloid Interface Sci. 235 (2016) 201–213.
[23] Huang Z, Raghuwanshi VS, Garnier G. Functionality of immunoglobulin g and immunoglobulin m antibody physisorbed on cellulosic films. Front Bioeng Biotechnol 5.
[24] J. Su, C.J. Garvey, S. Holt, R.F. Tabor, B. Winther-Jensen, W. Batchelor, G. Garnier, Adsorption of cationic polyacrylamide at the cellulose–liquid interface: a neutron reflectometry study, J. Colloid Interface Sci. 448 (2015) 88–99.
[25] J. Li, X. Li, S. Michielsen, Alternative method for determining the original drop volume of bloodstains on knit fabrics, Forensic Sci. Int. 263 (2016) 194–203.
[26] H.-C. Chang, Electrokinetic transport of red blood cells in microcapillaries, Electrophoresis 23 (2002) 2165–2173.
[27] C. Zhu, I. Dobryden, J. Ryden, S. Oberg, A. Holmgren, A.P. Mathew, Adsorption behavior of cellulose and its derivatives toward Ag(i) in aqueous medium: an AFM, spectroscopic, and DFT study, Langmuir 31 (45) (2015) 12390–12400.
[28] G. Vazquez, E. Alvarez, J.M. Navaza, Surface tension of alcohol water+ water from 20 to 50. degree. c, J. Chem. Eng. Data 40 (3) (1995) 611–614.

[29] D.R. Schuchard, J.C. Berg, Liquid transport in composite cellulose superabsorbent fiber networks, Wood Fiber Sci. 23 (3) (2007) 342–357.
[30] A. Nilghaz, L. Zhang, W. Shen, Coffee stains on paper, Chem. Eng. Sci. 129 (2015) 34–41.
[31] R.D. Deegan, O. Bakajin, T.F. Dupont, G. Huber, S.R. Nagel, T.A. Witten, Capillary flow as the cause of ring stains from dried liquid drops, Nature 389 (6653) (1997) 827–829.
[32] R. Chen, L. Zhang, D. Zang, W. Shen, Wetting and drying of colloidal droplets: Physics and pattern formation, in: Advances in Colloid Science, InTech, 2016.
[33] T. Young, An essay on the cohesion of fluids, Philos. Trans. R. Soc. Lond. 95 (1805) 65–87.
[34] D. Brutin, Droplet Wetting and Evaporation: from Pure to Complex Fluids, Academic Press, 2015.
[35] B.S. Westerlind, J.C. Berg, Surface energy of untreated and surface-modified cellulose fibers, J. Appl. Polym. Sci. 36 (3) (1988) 523–534.
[36] K. Niegelhell, M. Süßenbacher, J. Sattelkow, H. Plank, Y. Wang, K. Zhang, S. Spirk, How bound and free fatty acids in cellulose films impact nonspecific protein adsorption, Biomacromolecules 18 (12) (2017) 4224–4231.
[37] K.T. Hodgson, J.C. Berg, The effect of surfactants on wicking flow in fiber networks, J. Colloid Interface Sci. 121 (1) (1988) 22–31.
[38] Z. Yang, C. Zhang, Adsorption/desorption behavior of protein on nanosized hydroxyapatite coatings: a quartz crystal microbalance study, Appl. Surf. Sci. 255 (8) (2009) 4569–4574.